Pflugers Arch - Eur J Physiol (2011) 461:579–589
DOI 10.1007/s00424-011-0947-0

TRANSPORT PHYSIOLOGY

Rotavirus toxin NSP4 induces diarrhea by activation of TMEM16A and inhibition of Na^+ absorption

Jiraporn Ousingsawat · Myriam Mirza · Yuemin Tian · Eleni Roussa · Rainer Schreiber · David I. Cook · Karl Kunzelmann

Received: 29 October 2010 / Revised: 18 February 2011 / Accepted: 21 February 2011 / Published online: 12 March 2011

Abstract Rotavirus infection is the most frequent cause for severe diarrhea in infants, killing more than 600,000 every year. The nonstructural protein NSP4 acts as a rotavirus enterotoxin, inducing secretory diarrhea without any structural organ damage. Electrolyte transport was assessed in the colonic epithelium from pups and adult mice using Ussing chamber recordings. Western blots and immunocytochemistry was performed in intestinal tissues from wild-type and TMEM16A knockout mice. Ion channel currents were recorded using patch clamp techniques. We show that the synthetic $NSP4_{114–135}$ peptide uses multiple pro-secretory pathways to induce diarrhea, by activating the recently identified Ca^{2+}-activated Cl^- channel TMEM16A, and by inhibiting Na^+ absorption by the epithelial Na^+ channel ENaC and the Na^+/glucose cotransporter SGLT1. Activation of secretion and inhibition of Na^+ absorption by $NSP4_{114–135}$, respectively, could be potently suppressed by wheat germ agglutinin which probably competes with $NSP4_{114–135}$ for binding to an unknown glycolipid receptor. The present paper gives a clue as to mechanisms of rotavirus-induced diarrhea and suggests wheat germ agglutinin as a simple and effective therapy.

Keywords Rotavirus · NSP4 · Ca^{2+}-activated Cl^- channels · TMEM16A · ENaC · Epithelial Na^+ channels · SGLT1 · Colonic epithelium · Diarrhea

Introduction

Rotavirus is the major cause for infantile gastroenteritis that causes each year more than 600,000 deaths worldwide [5, 25]. The rotavirus nonstructural glycoprotein NSP4 and the synthetic peptide $NSP4_{114–135}$ have been demonstrated to cause diarrhea in rodents aged 10–14 days [3, 27]. Infected intestinal cells release NSP4 into the intestinal lumen, where it acts as a viral toxin inducing Ca^{2+}-dependent Cl^- secretion, and inhibition of the Na^+/glucose-cotransporter SGLT1 [13, 27]. Thus, glucose malabsorption and activation of cystic fibrosis conductance regulator (CFTR)-independent Cl^- secretion may be the cause for diarrhea. It is thought that NSP4 binds to a yet unidentified apical membrane receptor, activates phospholipase C (PLC), and enhances intracellular Ca^{2+} by causing release from intracellular Ca^{2+} stores, as demonstrated in cultured HT_{29} and CaCo-2 cells [4, 9]. While early effects of NSP4 are due to PLC and Ca^{2+} release from ER store, late effects are due to disorganization of the actin cytoskeleton and continuous increase of intracellular Ca^{2+} by both ER Ca^{2+} release and influx of extracellular Ca^{2+} [4].

The contribution of Cl^- secretion to rotavirus-related diarrhea has been discussed controversially, and the role of other transport mechanisms is under debate [2, 3, 24, 25]. A striking observation was that NSP4 induces diarrhea in neonatal cystic fibrosis mice lacking expression of CFTR,

Electronic supplementary material The online version of this article (doi:10.1007/s00424-011-0947-0) contains supplementary material, which is available to authorized users.

J. Ousingsawat · M. Mirza · Y. Tian · R. Schreiber · K. Kunzelmann (✉)
Institut für Physiologie, Universität Regensburg, Universitätsstraße 31,
93053 Regensburg, Germany
e-mail: karl.kunzelmann@vkl.uni-regensburg.de

D. I. Cook
Department of Physiology, University of Sydney,
2006 Sydney, NSW, Australia

E. Roussa
Department of Anatomy, University of Freiburg,
79100 Freiburg, Germany

through the activation of an age- and Ca^{2+}-dependent plasma membrane anion permeability distinct from CFTR [27]. We identified that mice lacking expression of the recently identified Ca^{2+}-dependent Cl^- channel TMEM16A [6, 36, 42] do not show Ca^{2+}-dependent Cl^- secretion in the colon [29]. Thus, TMEM16A, possibly along with other members of the TMEM16 family, is likely to form the apical Ca^{2+}-dependent Cl^- channel in mouse intestinal epithelium. This result and our previous findings showing that hemagglutinin from influenza virus inhibits the epithelial Na^+ channel (ENaC) by a phospholipase C and protein kinase C-dependent mechanism [16] prompted the present study. We examined the effect of $NSP4_{114–135}$ on ion transport in the mouse colonic epithelium, which is able to secrete Cl^- and absorb Na^+ through ENaC and the Na^+/glucose cotransporter (SGLT1).

Previous work indicated that exposure of epithelial tissues to virus proteins can inhibit the ENaC, which is likely to contribute to the pathogenesis of viral diseases [16, 19]. As ENaC is not expressed in the small intestine but only in the colon, we decided to use the colonic epithelium for our study, since it expresses many of the important channels and transporters that could be targeted by intestinal pathogens [18]. Moreover, since age dependence of the rotavirus infection has been reported previously [3], we decided to examine the effects of $NSP4_{114–135}$ at different ages. We show that both transport by ENaC and SGLT1 are inhibited by rotavirus toxin, while TMEM16A Cl^- channels are activated. We further find that these effects of $NSP4_{114–135}$ can be blocked by wheat germ agglutinin. Our findings suggest TMEM16A [8], ENaC [22], and SGLT1 as pharmacological targets in rotavirus-induced diarrhea.

Material and methods

Animals and Ussing chamber experiments Neonatal (1–3 days), juvenile (10–14 days), and young adult (30–40 days) C57BL/6 mice were killed after exposure to Isofluran (Baxter, Germany), and the proximal/distal colon was removed. The stripped colon was put into ice cold Ringer bath solution (mM: NaCl 145, KH_2PO_4 0.4, K_2HPO_4 1.6, D-glucose 6, $MgCl_2$ 1, Ca-gluconate 1.3, pH 7.4) containing indomethacin (10 μM). Tissues were mounted into a micro-perfused Ussing chamber with a circular aperture of 0.785 mm^2. Luminal and basolateral sides of the epithelium were perfused continuously at a rate of 5 ml/min. Bath solutions were heated to 37°C, using a water jacket. Experiments were carried out under open circuit conditions. Data were collected continuously using PowerLab (AD Instruments, Australia). Values for transepithelial voltages (V_{te}) were referred to the serosal side of the epithelium. Transepithelial resistance (R_{te}) was determined by applying short (1 s) current pulses (ΔI=0.5 μA). R_{te} and equivalent short circuit currents (I'_{SC}) were calculated according to Ohm's law ($R_{te} = \Delta V_{te}/\Delta I$, $I'_{SC} = V_{te}/R_{te}$). Experiments in M1 cells were performed under short circuit conditions (I_{sc}).

Transfection and patch clamp HEK293 cells were transfected with human TMEM16A (accession number NP_060513) or empty plasmid. TMEM16A (isoform abc, according to Caputo et. al. [6]) was subcloned into pcDNA3.1 V5-His (Invitrogen, Karlsruhe, Germany). Plasmids were transfected into HEK293 cells using standard methods (lipofectamine, Invitrogen, Karlsruhe, Germany). Control transfections were done with the empty pcDNA3.1 vector. The transfection efficacy was around 80%. Transfected cells were identified using cotransfected pIRES1-CD8 and Dynabeads M-450 CD8 (Dynal Biotech, Norway). All experiments were performed 48 h after the transfection.

Cells grown on cover slips were mounted in a perfused bath on the stage of an inverted microscope (IM35, Zeiss) and kept at 37°C. The bath was perfused continuously with Ringer solution (mM: NaCl 145, KH_2PO_4 0.4, K_2HPO_4 1.6, D-glucose 6, $MgCl_2$ 1, Ca-gluconate 1.3, pH 7.4) at about 10 ml/min. Patch-clamp experiments were performed in the fast whole-cell configuration. Patch pipettes had an input resistance of 2–4 MΩ, when filled with an intracellular-like solution containing (mM) KCl 30, K-gluconate 95, NaH_2PO_4 1.2, Na_2HPO_4 4.8, EGTA 1, Ca-gluconate 0.758, $MgCl_2$ 1.034, D-glucose 5, ATP 3. pH was 7.2, the Ca^{2+} activity was 0.1 μM. The access conductance was measured continuously and was 60–140 nS (EPC 7 amplifier, List Medical Electronics, Darmstadt, Germany). In regular intervals, membrane voltages (V_c) were clamped in steps of 10 mV from −50 to +50 mV and the membrane conductance G_m was calculated from the measured current (I) and V_c values according to Ohm's law.

Real-time RT-PCR Total RNA was isolated from mouse colon (C57BL/6; three mice) using RNeasy Mini-Kit (Qiagen; Hilden, Germany) and reverse-transcribed for 1 h at 37°C. Real-time RT-PCR was performed in a plate reader Light Cycler 480 (Roche Applied Science, Germany) using Sybrgreen (Roche Applied Science, Germany) and primers as shown in Supplementary Table 1. To compare different runs, a calibrator was used. Amplification was followed by melting curve analysis, and data were analyzed with Light Cycler 480 software by normalizing to β-actin expression. Mean and SEM values were calculated from three independent runs. As negative controls, water instead of cDNA was run with every PCR. Products were further analyzed on ethidium bromide-stained 2% agarose gels.

Western blotting Tissues were isolated from WT and KO pups and adult mice (S129 and C57BL/6), placed into cold ringer solution and homogenized in RIPA buffer (1% Triton X-100, 0.01% SDS, 150 mM NaCl, 20 mM Tris–HCl pH 7.5, 0.08% deoxycholic acid, 5 U/ml Benzonase + protease inhibitor) as frozen tissues. Protein was separated using PAGE (8%), transferred to PVDF membranes (Millipore), and probed overnight at 4°C with a rabbit polyclonal anti-mTMEM16a antibody (generous gift by Dr. B. Harfe, University of Gainesville, FL, USA). Blots were visualized using a secondary HRP-conjugated anti-rabbit AB (Acaris, R136HRP) and chemiluminescence (Pierce).

Immunohistochemistry of TMEM16A Animals were perfused transcardially with 4% PFA in PBS. Colon tissues were dehydrated, embedded in paraffin, and cut; 10 μm tissue sections were mounted on Superfrost Plus adhesive glass slides, deparaffinized in xylene, rehydrated in graded ethanol, and washed with PBS. Subsequently, sections were placed into 0.1 M citrate buffer and heated in a microwave oven for 10 min at approximately 600 W for antigen retrieval. Slides were washed with PBS, blocked for 2 h (10% NGS and 0.1% Triton-X-100), and incubated with polyclonal anti-TMEM16A AB (1:800; ON at 4°C). Sections were incubated with biotinylated secondary goat-anti-rabbit AB (Sigma Aldrich, Taufkirchen, Germany; 1:200 for 1 h at RT) and incubated with FITC-coupled streptavidin (1:200; 30 min at RT). Immunofluorescence was recorded using a confocal laser scanning microscope (Zeiss LSM 510 Meta, Carl Zeiss MicroImaging GmbH, Jena) using 488 nm laser excitation.

Materials and statistical analysis All compounds used were of highest available grade of purity. DIDS, amiloride, pertussis toxin (PTX), pertussis toxin B oligomer/binding protein (PTX-BP), bisindolylmaleimide (BIM), indomethacin, carbachol, cyclopiazonic acid (CPA), and ATP were from SIGMA (Taufkirchen, Germany). U73122 was from Merck/Calbiochem (Nottingham, UK). For the present experiments, a synthetic $NSP4_{114–135}$ peptide was used. Not all rotaviruses cause severe diarrhea in mice since their virulence depends on the amino acid sequence of NSP4 [44]. The $NSP4_{114–135}$ peptide used in this study corresponds to the active core of NSP4 of the simian virus strain SA11. It has been shown to induce diarrhea in mice in an age- and dose-dependent fashion, in the absence of histological alterations [2, 3, 27]. The $NSP4_{114–135}$ peptide (Ac-DKLTTREIEQVELLKRIYDKLT-NH2) was from Mimotopes (Clayton, Australia). Scrambled control peptide or unrelated peptides of random sequence (con pep) were used as controls. Student's *t* test (for paired or unpaired samples as appropriate) was used for statistical analysis. $P<0.05$ was accepted as significant.

Results

Activation of Cl^- secretion by $NSP4_{114–135}$ in mouse colon Colonic tissues were removed from mice of different ages, and basal bioelectric properties were assessed (Table 1). The $NSP4_{114–135}$ rotavirus enterotoxin was applied to the luminal side of stripped 10–14 days postnatal mouse colon, at concentrations ranging from 0.1 to 5 μM. $NSP4_{114–135}$ induced a partially transient negative transepithelial voltage deflection in open-circuit Ussing chamber recordings, suggesting stimulation of Cl^- secretion due to activation of luminal Cl^- channels (Fig. 1a). The effects of NSP4 varied from tissue to tissue. In most cases (79%), the response was steady, but in 21%, it was transient. In contrast, application of scrambled control peptide (con pep) had no effect on colonic ion transport (Fig. 1a). Calculation of the maximal equivalent short circuit currents (I'_{sc}) indicated a dose-dependent activation of ion transport by $NSP4_{114–135}$ (Fig. 1b). Maximal $NSP4_{114–135}$-induced ion transport (Cl^- secretion) was in the range of 25 $\mu A/cm^2$. For comparison, forskolin, a strong activator of CFTR, induced around 50 $\mu A/cm^2$ in the present and in previous reports (data not shown) [3]. We, therefore, would assume that the effects of $NSP4_{114–135}$ on colonic ion transport correlate to a diarrheic effect.

Since age dependence of the rotavirus infection has been reported previously [3], we decided to examine the effects of $NSP4_{114–135}$ at different ages. We compared activation of ion transport by $NSP4_{114–135}$ (5 μM) in the neonatal colon (1–3 days old) with that of mice aging 10–14 and 30–40 days, respectively (Fig. 1c). While little Cl^- secretion induced by $NSP4_{114–135}$ was observed in the neonatal colon, both proximal and distal colon of juvenile mice (10–14 days) showed the strongest Cl^- secretion upon exposure to $NSP4_{114–135}$, which declines as animals grow older (30–40 days). In contrast, Cl^- secretion induced in the proximal colon by stimulation of basolateral cholinergic receptors with carbachol (CCH; 100 μM) was more pronounced than that induced by $NSP4_{114–135}$ (Fig. 2b) and was similar in neonatal, juvenile, and adult colon (data not shown). Notably, the juvenile distal colon exhibit a pronounced Cl^- secretion upon stimulation with CCH (43.3±5.3 $\mu A/cm^2$; $n=13$), which is not detected in the adult distal colon

Table 1 Basal bioelectric properties of mouse colon at different ages

Age	Number	R_{te} (Ω cm^2)	V_{te} (mV)	I'_{sc} ($\mu A/cm^2$)
Neonatal (1–3 days)	15	29.9±1.9	−0.9±0.2	21.7±1.7
Juvenile (10–14 days)	22	31.2±2.1	−1.9±0.2	50.2±6.1
Adult (30–40 days)	24	31.3±1.7	−3.1±0.3	60.2±4.8

R_{te} transepithelial resistance, V_{te} transepithelial voltage, I'_{sc} equivalent short circuit current

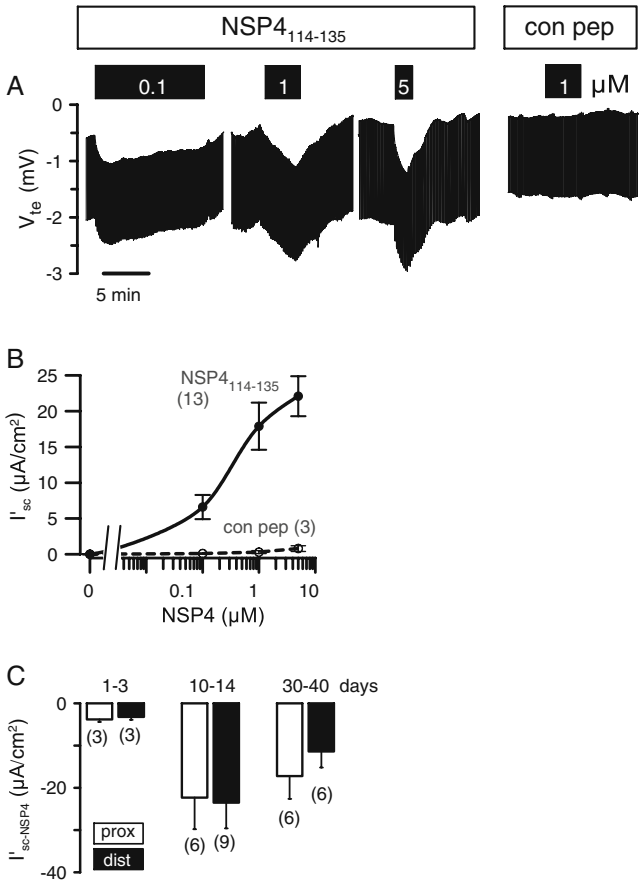

Fig. 1 Activation of Cl^- secretion by $NSP4_{114–135}$: **a** Ussing chamber recordings of the V_{te} measured in mouse colon. The mucosal side of distal colon from a neonatal mouse was exposed to increasing concentrations of $NSP4_{114–135}$ (µM), which caused negative voltage deflections indicating activation of Cl^- secretion. **b** Concentration dependent activation of equivalent short circuit currents (I_{sc}) in distal colon by $NSP4_{114–135}$. Application of scrambled con pep had no effect on colonic ion transport. **c** $NSP4_{114–135}$-induced short circuit currents in proximal and distal colon from neonatal (1–3 days), postnatal (10–14 days), and young adult mice (30–40 days). Mean ± SEM, (*n*) = number of tissues measured. *Asterisk* indicates significant difference (paired *t* test)

(0.2±0.01 µA/cm^2; n=11) [32]. Thus, Ca^{2+}-dependent Cl^- secretion in mouse colon varies with age and is different for $NSP4_{114–135}$ and hormone-dependent stimulation.

NSP4 activates Ca^{2+}-dependent Cl^- secretion $NSP4_{114–135}$ was reported to activate Ca^{2+}-dependent Cl^- channels in the apical membrane of colonic epithelial cells, which is independent of CFTR [3, 27]. In fact, after suppression of CFTR by inhibition of prostaglandin synthesis with 10 µM indomethacin [18], Cl^- secretion was readily activated by either $NSP4_{114–135}$ (5 µM) or the muscarinic agonist carbachol (100 µM), indicating the existence of a luminal Cl^- channels independent of CFTR (Fig. 2a). We did not use $CFTR_{inh}172$ or GlyH-101 to block CFTR, since we found that these inhibitors were not very effective in mouse colon (data not shown). In contrast to CCH-activated transport, $NSP4_{114–135}$-induced Cl^- secretion was remarkably less transient. We found that 5 µM carbachol produced similar equivalent short circuit currents (24.8±3.8 µA/cm^2; n=6) as 5 µM $NSP4_{114–135}$. Activation of Cl^- secretion by both $NSP4_{114–135}$ and carbachol was inhibited by DIDS (200 µM; Fig. 2b). Thus, both $NSP4_{114–135}$ and CCH seem to activate the same type of Ca^{2+}-activated Cl^- channel. Surprisingly, when ER Ca^{2+} stores were depleted with CPA (10 µM), activation of Cl^- secretion by $NSP4_{114–135}$ was abolished while CCH-induced secretion was even enhanced (Fig. 2c). Moreover, inhibition of phospholipase C with U73122 (10 µM) inhibited $NSP4_{114–135}$-activated Cl^- secretion but augmented CCH-induced secretion (Fig. 2d). Luminal $NSP4_{114–135}$, therefore, activates Cl^- secretion in a Ca^{2+}-dependent manner and relies on IP_3-dependent Ca^{2+} release from luminal ER Ca^{2+} stores, while basolateral CCH may utilize mechanisms that comprise phosphoinositide 3-kinase and probably mitogen-activated protein kinase, as suggested earlier for CCH activation of luminal K^+ secretion [32].

Stimulation of luminal purinergic receptors in the distal colon of adult mice is known to activate large conductance Ca^{2+}-dependent K^+ channels [32, 34]. We compared the effects of luminal ATP (100 µM) with that of $NSP4_{114–135}$ in distal postnatal colon. The experiments were performed in the presence of amiloride to exclude secondary effects on ENaC. Interestingly, ATP activated a pronounced yet transient K^+ secretion that was followed by Cl^- secretion. In contrast, $NSP4_{114–135}$ activated only a Cl^- secretion that was larger than that produced by ATP (Fig. 2e, f). These results suggest that $NSP4_{114–135}$ may not only increase intracellular Ca^{2+} and thereby activate Ca^{2+}-dependent Cl^- secretion but may also have additional effects distal to the Ca^{2+} rise, maybe by directly activating Ca^{2+}-dependent Cl^- channels, a mechanism that had been proposed earlier [26].

Expression of TMEM16A in mouse colon and activation by NSP4 Recently, TMEM16A has been identified as a major component of Ca^{2+}-activated Cl^- channels [6, 36, 42]. TMEM16A (anoctamin 1, ANO1) belongs to a family of 10 TMEM16 proteins (TMEM16A-K, ANO 1–10). TMEM16A exhibits ion channel properties that truly reflect those of endogenous Ca^{2+}-dependent Cl^- channels. We recently demonstrated defective Ca^{2+}-dependent Cl^- secretion in distal colon and other epithelial organs of mice lacking TMEM16A. These results strongly suggest that TMEM16A is the intestinal luminal Ca^{2+}-dependent Cl^- channel in mouse colon [1, 29]. We, therefore, analyzed expression of TMEM16A and other TMEM16 proteins in mouse colon. Using quantitative real-time PCR, we found pronounced expression of TMEM16A (ANO1) in distal but not proximal colon along with a number of other TMEM16

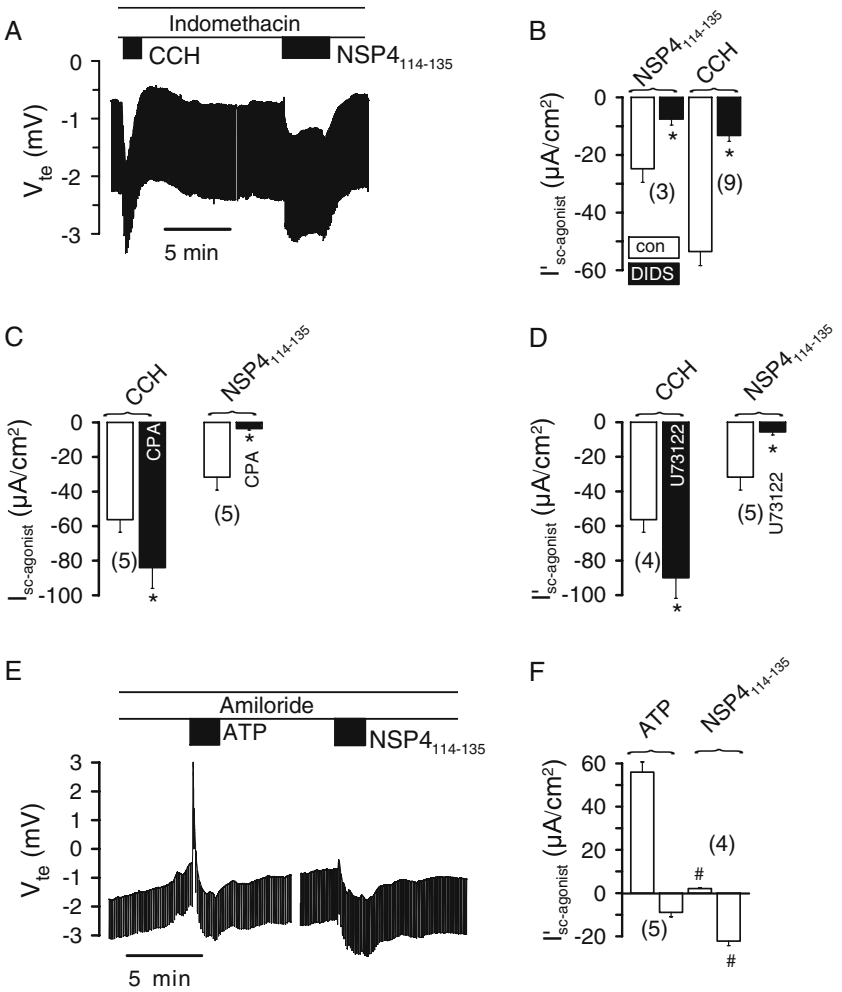

Fig. 2 $NSP4_{114–135}$ activates Ca^{2+}-dependent Cl^- secretion: **a** Ussing chamber recording of the V_{te} measured in mouse postnatal distal colon incubated in indomethacin (10 μM) to inactivate endogenous CFTR. CCH (100 μM) induced a transient voltage deflection, while $NSP4_{114–135}$ (5 μM) induced a smaller but less transient voltage deflection. **b** Calculation of I_{sc} indicated activation of Cl^- secretion by $NSP4_{114–135}$ and CCH, which was both inhibited by luminal application of the inhibitor of Ca^{2+}-activated Cl^- channels DIDS (200 μM). **c** Depletion of ER-Ca^{2+} stores by CPA (10 μM) largely reduced $NSP4_{114–135}$-induced I_{sc}, while CCH-induced secretion was augmented. **d** Inhibition of phospholipase C by U73122 (10 μM) largely reduced $NSP4_{114–135}$-induced I_{sc}, while CCH-induced secretion was augmented. **e** Activation of ion transport in mouse distal postnatal colon by stimulation of luminal purinergic receptors with ATP (100 μM) and $NSP4_{114–135}$. While ATP caused a biphasic response due to initial activation of K^+ secretion (positive voltage deflection) followed by a small negative deflection due to activation of Cl^- secretion, $NSP4_{114–135}$ only activated a Cl^- secretion. Na^+ absorption through ENaC was inhibited by amiloride (10 μM). **f** Summary of the ion transport activated by ATP and $NSP4_{114–135}$. Mean ± SEM, (n) = number of tissues measured. *Asterisk* indicates significant difference (paired *t* test). *Number sign* indicates significant difference (unpaired *t* test)

proteins (Fig. 3a). Notably, expression of both a short and long form of TMEM16J (ANO9) was detected in the proximal colon of adult mice. Transcripts for other TMEM16 proteins were either not detected or were only present at negligible copy numbers. Expression of TMEM16A in adult distal mouse colon and lack of expression in proximal colon was confirmed by Western blotting (Fig. 3b, left panel). Expression of ANO1 was also found in colon and ileum of pups but was missing in the intestine of mice lacking expression of TMEM16A (ANO1) [29, 33]. Only a faint band was detected in the lysates from colon of null mice which is probably due to cross-reactivity with other anoctamins expressed in the colonic epithelium. Apart from ANO1, we detected expression of a number of other anoctamins in mouse colonic epithelium such as ANO6, ANO9, and ANO10 [35]. Immunocytochemistry of TMEM16A indicated expression in both the apical and basolateral compartment of colonic epithelial cells, as suggested earlier [29] (Fig. 3c).

We examined whether TMEM16A is activated by $NSP4_{114–135}$, when expressed in HEK293 cells. As shown in Fig. 4a, no whole-cell currents were activated by exposure of mock transfected (control) cells to the rotavirus enterotoxin $NSP4_{114–135}$ (1 μM). In contrast, exposure of

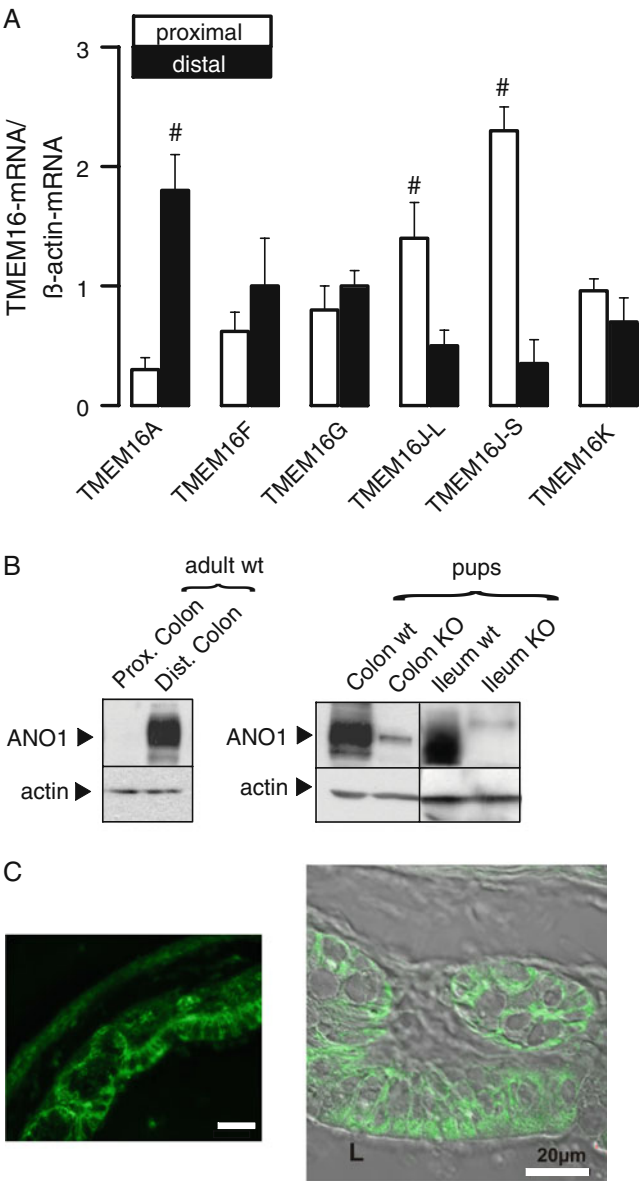

Fig. 3 Expression of TMEM16A in mouse colon: **a** Quantitative real-time RT-PCR analysis of expression of TMEM16 proteins in mouse colon. Expression of TMEM16A was dominant in the distal colon. **b** Western blot analysis of TMEM16A in mouse proximal and distal colon indicates pronounced expression in the distal colon with little expression in the proximal colon. **c** Immunohistochemistry of TMEM16A in mouse distal colon of TMEM16A+/+ (WT) and TMEM16A−/− (KO) mice. Marker=50 µm. Mean ± SEM, (n) = number of tissues measured. *Number sign* indicates significant difference between proximal and distal colon (unpaired *t* test)

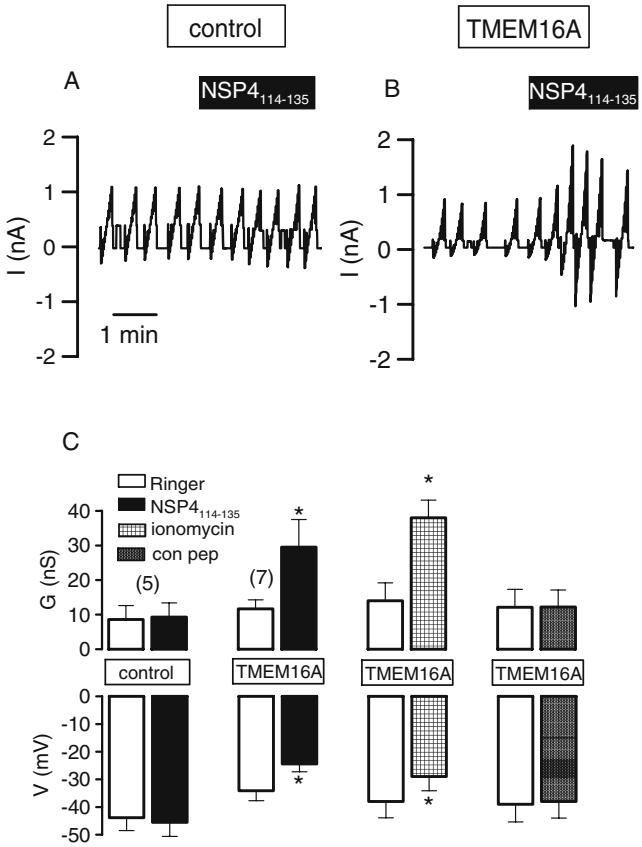

Fig. 4 Activation of TMEM16A by $NSP4_{114–135}$: **a**, **b** Original recording of the whole cell current in mock transfected (**a**) and TMEM16A expressing (**b**) HEK293 cells. $NSP4_{114–135}$ (1 µM) activates a whole-cell Cl^- current in TMEM16A-expressing cells. **c** Summary of the whole-cell conductances activated by $NSP4_{114–135}$. In TMEM16A expressing cells but not in control cells, $NSP4_{114–135}$ depolarizes the membrane voltage by activation of a whole-cell Cl^- conductance. Unrelated con pep had no effect on whole-cell currents, while increase in intracellular Ca^{2+} by ionomycin also activated TMEM16A (Fig. 1a, b). Mean ± SEM, (n) = number of tissues measured. *Asterisk* indicates significant difference (paired *t* test)

TMEM16A-expressing HEK293 cells to $NSP4_{114–135}$ induced a whole-cell Cl^- current and conductance (Fig. 4b, c). A whole-cell Cl^- current was also activated by increase in intracellular Ca^{2+} using the Ca^{2+} ionophore ionomycin (1 µM) as a positive control. In contrast, no current was activated by an unrelated control peptide (Fig. 4c). The NSP4 enterotoxin may, therefore, activate Ca^{2+}-dependent Cl^- channels through increase of intracellular Ca^{2+} and perhaps directly through direct binding to TMEM16A, as proposed earlier [26]. Moreover, no current was elicited by NSP4 in CFTR-expressing cells; in contrast, NSP-induced currents were somewhat reduced in cells co-expressing TMEM16A and CFTR (data not shown).

Inhibition of Na^+ transport by $NSP4_{114–135}$ We examined whether increase in intestinal net secretory transport by $NSP4_{114–135}$ is also due to parallel inhibition of salt absorption. Direct inhibition of Na^+/glucose-cotransport by $NSP4_{114–135}$ has been demonstrated recently in rabbit intestinal brush border [13]. In Ussing chamber recordings, we analyzed the effects of isotonic replacement of luminal mannitol by glucose (gluc; 20 mM) on the transepithelial voltage. Application of glucose leads to a negative voltage deflection indicating the transport activity of the intestinal

electrogenic Na^+/glucose cotransporter SGLT (Fig. 5a). The effect of glucose on V_{te} and activation of I_{sc} was blunted in the presence of $NSP4_{114–135}$, indicating inhibition of electrogenic Na^+/glucose cotransport (Fig. 5a, b). To further confirm expression of SGLT in mouse colon, we performed RT-PCR analysis and found SGLT1 (SLC5a1) but not SGLT2 (SLC5a2) expressed in both proximal and distal colon (Fig. 5c).

Our previous work indicated that electrogenic Na^+ absorption through amiloride-sensitive Na^+ channels (ENaC) is inhibited by bacterial components as well as viral coat proteins [16, 17, 19, 20]. Here, we examined whether inhibition of ENaC is also observed for the rotavirus enterotoxin $NSP4_{114–135}$. Electrogenic Na^+ absorption is readily observed in distal colon of postnatal mouse as indicated by an amiloride-induced change in the transepithelial voltage (Fig. 5d). After exposure of distal colon to $NSP4_{114–135}$, the effect of amiloride was attenuated, and amiloride-sensitive I'_{sc} ($I'_{sc\text{-}ENaC}$) was inhibited (Fig. 5d, e). Importantly, scrambled control peptide (con pep) had no effects on either SGLT1 or ENaC (Fig. 5b, e).

However, assessment of $I'_{sc\text{-}ENaC}$ and $I'_{sc\text{-}SGLT1}$ may not be correct in the presence of $NSP4_{114–135}$-induced Cl^- conductance. We, therefore, made use of the specific inhibitor of Ca^{2+}-activated Cl^- currents, AO1 (20 μM) [8]. AO1 completely blocked $NSP4_{114–135}$-activated Cl^- transport (−AO1: $\Delta I'sc_{NSP4}=22.3\pm8$ μA/cm^2; $n=6$ vs. +AO1: $\Delta I'sc_{NSP4}=0.2\pm0.01$ μA/cm^2; $n=4$). We again examined the effects of $NSP4_{114–135}$ on $I'_{sc\text{-}ENaC}$ and $I'_{sc\text{-}SGLT1}$, but this time in the presence of AO1 (Fig. 5f): Both amiloride (Amil) and glucose removal (−G) significantly reduced I'_{sc} in the absence of $NSP4_{114–135}$. While

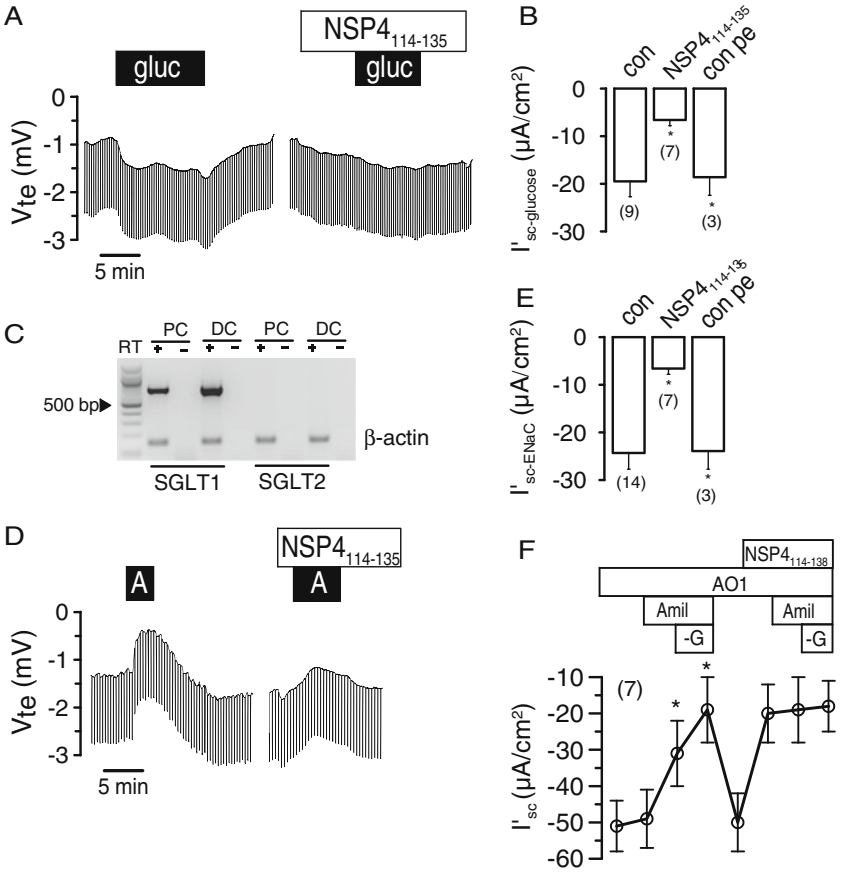

Fig. 5 Inhibition of Na^+ transport by $NSP4_{114–135}$: **a** Ussing chamber recording of the effects of luminal application of glucose (gluc; 20 mM) on V_{te}, in the absence and presence of $NSP4_{114–135}$ (5 μM). Application of glucose leads to a negative voltage deflection indicating the transport activity of the Na^+/glucose cotransporter SGLT1. The effect of glucose was blunted in the presence of $NSP4_{114–135}$. **b** Summary of the glucose induced equivalent short circuit currents before and after exposure to $NSP4_{114–135}$. **c** RT-PCR analysis of the expression of SGLT1 (SLC5a1) and SGLT2 (SLC5a2) in proximal (*PC*) and distal (*DC*) colon. **d** Ussing chamber recording of the effect of amiloride (*A*; 10 μM) on V_{te}, in the absence and presence of $NSP4_{114–135}$ (5 μM). Application of amiloride leads to a positive voltage deflection indicating inhibition of ENaC by amiloride. The effect of amiloride was reduced after application of $NSP4_{114–135}$. **e** Summary of Na^+ transport by ENaC before and after exposure to $NSP4_{114–135}$. Scrambled con pep had no effects on either SGLT1 or ENaC. **f** Summary of the effects of amiloride (*Amil*), glucose (20 mmol/l) removal (−G), and $NSP4_{114–135}$ exposure on equivalent short circuit currents. No effects of $NSP4_{114–135}$, amiloride, or glucose removal were observed in the presence of the CaCC inhibitor AO1 (20 μM). Mean ± SEM, (n) = number of tissues measured. *Asterisk* indicates significant difference (paired *t* test)

application of $NSP4_{114–135}$ in the presence of AO1 reduced I'_{sc}, no further effects of amiloride or glucose removal were observed. These experiments suggest that $NSP4_{114–135}$ truly inhibits Na^+ transport by ENaC and SGLT1. Moreover, a significant inhibition of $I_{sc\text{-}ENaC}$ from 20.3±2.5 μA/cm^2 (−$NSP4_{114–135}$) to 8.7±1.6 μA/cm^2 (+NSP4; n=5) was found in mouse M1 collecting duct cells when measured under real short circuit (not open circuit) conditions. We conclude that NSP4 may induce intestinal net electrolyte secretion and secretory diarrhea by both activation of Cl^- secretion and inhibition of Na^+ absorption.

Mechanisms for activation of intestinal electrolyte secretion We further examined the mechanisms by which rotavirus enterotoxin may activate Cl^- secretion. Previous reports on Cl^- secretion induced by other pathogens such as influenza virus or Sendai virus indicated a role of GTP-binding proteins and downstream enzymes such as phospholipase C [7, 16, 17]. In fact, when $NSP4_{114–135}$ was applied in the presence of the inhibitor of Gi/o proteins, pertussis toxin (300 ng/ml for 3 h), activation of Cl^- secretion by $NSP4_{114–135}$ ($I_{sc\text{-}NSP4}$) was reduced, although not completely inhibited (Fig. 6a). Additional inhibition of protein kinase C by BIM (100 nM) did not further reduce $I_{sc\text{-}NSP4}$, indicating that protein kinase C is irrelevant for the activation of Cl^- secretion. This has also been found previously for parainfluenza-induced Cl^- secretion [17]. In contrast, both PTX and inhibition of PKC by BIM enhanced Cl^- secretion activated by the secretagogue CCH (Fig. 6b). This result points to fundamental differences in cell signaling for rotavirus enterotoxin and hormone-induced Cl^- secretion,

Influenza virus has been shown earlier to inhibit epithelial Na^+ channels through activation of protein kinase C. We, therefore, examined the effects of $NSP4_{114–135}$ on Na^+ absorption in the presence of the PKC-inhibitor BIM. In fact, Na^+ absorption by either ENaC or SGLT1 was no longer inhibited by $NSP4_{114–135}$ after inhibition of PKC by BIM (Fig. 6c). Moreover, the membrane-binding domain of PTX (PTX-BP; B-oligomer), which is a known activator of PKC, also inhibited Na^+ transport by ENaC and SGLT1 [16]. We conclude that binding of NSP4 to an unknown membrane receptor leads to activation of phospholipase C, increase of intracellular Ca^{2+}, and activation of PKC.

The intestinal membrane receptor for NSP4 has not yet been identified; however, it is likely that it binds to a glycolipid or glycoprotein moiety of a lectin receptor, as suggested for other pathogens [16]. Since lectin-binding can be antagonized by monosaccharides, we also examined the effects of $NSP4_{114–135}$ on Cl^- secretion in the presence of luminal wheat germ agglutinin (WGA; 100 μg/ml; 20 min). WGA itself did not activate Cl^- secretion ($I_{sc\text{-}Cl}$-) but largely reduced Cl^- secretion activated by $NSP4_{114–135}$ (5 μM; Fig. 6d). Moreover, electrogenic Na^+ absorption by both ENaC ($I_{sc\text{-}ENaC}$) and SGLT1 ($I_{sc\text{-}glucose}$; Fig. 6d) were no longer inhibited by $NSP4_{114–135}$ in the presence of WGA. Moreover, WGA has no intrinsic effects on ion transport in the colon [22]. Moreover, WGA was found to inhibit membrane uptake of Shigella toxin and has been suggested for its anti-diarrheic effects [15]. However, WGA does not seem the only agglutinin that interferes with the rotavirus effects, as soy bean agglutinin, for which we found no prosecretory effects in the colon [22], also inhibited $NSP4_{114–135}$-induced transport significantly by 42±5.2% (n=5). Thus,

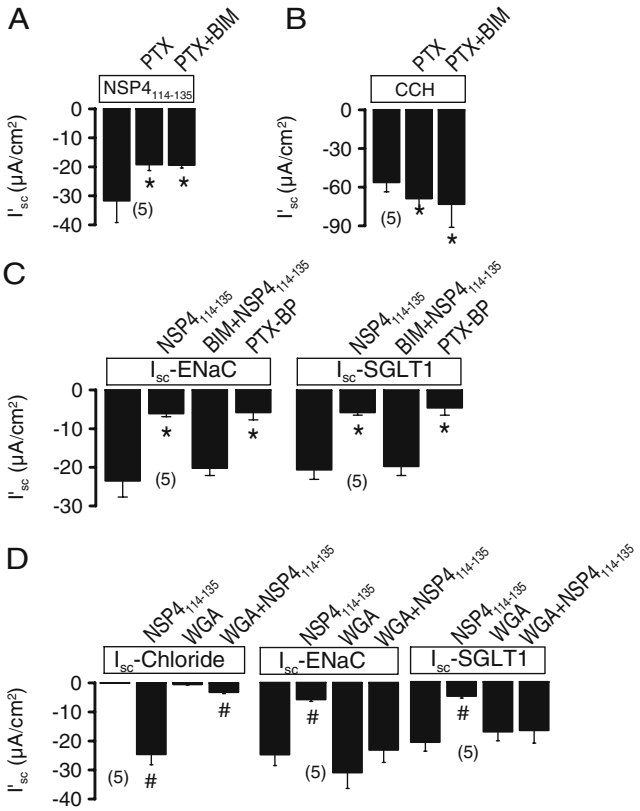

Fig. 6 Mechanisms by which $NSP4_{114–135}$ affects ion transport: **a** Summary of $NSP4_{114–135}$-induced Cl^- secretion ($I_{sc\text{-}NSP4}$) under control conditions (con) and after incubation of the tissue with pertussis toxin (*PTX*; 300 ng/ml/20 min) or PTX in the presence of the protein kinase C inhibitor BIM (0.1 μM). **b** Summary of CCH-induced Cl^- secretion ($I_{sc\text{-}CCH}$) under control conditions (con) and after incubation of the tissue with pertussis toxin (*PTX*; 300 ng/ml/20 min) or PTX in the presence of the protein kinase C inhibitor BIM (0.1 μM). **c** Summary of the amiloride sensitive Na^+ transport by ENaC ($I_{sc\text{-}ENaC}$) and the electrogenic glucose transport by SGLT1 ($I_{sc\text{-}glucose}$) under control conditions, after exposure to $NSP4_{114–135}$ (5 μM) in the presence of BIM (0.1 μM), and after exposure to the membrane binding component of pertussis toxin (PTX-BD, B-oligomer, 300 ng/ml/20 min). **d** Ca^{2+}-activated Cl^- secretion, Na^+ transport by ENaC, and glucose transport by SGLT1 in the presence of luminal WGA (100 μg/ml; 20 min) and in the presence of both $NSP4_{114–135}$ (5 μM) and WGA. Mean ± SEM, (n) = number of tissues measured. *Asterisk* indicates significant difference (paired t test). *Number sign* indicates significant difference (unpaired t test)

NSP4 is causing secretory diarrhea by inducing multiple changes in electrogenic ion transport. These NSP4 effects may be effectively antagonized effectively by simple oral treatment with wheat germ or simple monosaccharides.

Discussion

Ca^{2+}-dependent Cl^- secretion The present data indicate similar basal transport properties in neonatal, juvenile, and adult colon. They are in good agreement with results obtained in previous studies [12, 32]. In contrast to adult mice where Ca^{2+}-activated Cl^- secretion was only observed in the proximal colon, young animals show pronounced carbachol-activated Cl^- secretion also in the distal colon. This Cl^- transport is clearly independent of CFTR [32]. It should be kept in mind, however, that a significant variability exists regarding transport properties in the colon of different mouse strains [10]. The present data indicate that Ca^{2+}-dependent ion transport, particularly Cl^- secretion induced by $NSP4_{114–135}$, varies with age (Fig. 1c). We found that the juvenile colon demonstrated the strongest pro-secretory effect when stimulated with $NSP4_{114–135}$, which then declines to lower values as the mouse is aging. According to the paper by Ball et al. [27], the strongest secretory effects of NSP4 were observed in mice aging 7–14 days, which fits well to the pronounced pro-secretory effect observed in 10–14 days old mice in our study. Our data also fully match the observations published for humans, since it is known that rotavirus causes diarrhea preferentially in small infants (from a few month of age up to a few years).

Previous reports and the present data demonstrate that $NSP4_{114–135}$ activates a Cl^- conductance that is Ca^{2+}-dependent but CFTR-independent [3, 27]. TMEM16A (anoctamin 1) is expressed together with other members of the TMEM16 family in colonic epithelial cells (Fig. 3). As shown earlier, TMEM16A-null mice lack of Ca^{2+}-dependent Cl^- secretion in the colon [29]. Thus, TMEM16A appear to be an essential component of luminal Ca^{2+}-activated Cl^- channels and contributes to basolateral volume regulated Cl^- channels in mouse colon [1, 29]. TMEM16A inhibitors may, therefore, be ideal to combat rotavirus-induced diarrhea [8].

Does NSP4 activate Cl^- secretion through increase of intracellular Ca^{2+}? The reported EC_{50} for NSP4-induced Ca^{2+} increase in HT_{29} cells was around 5 nM [9], which is markedly lower than the EC_{50} for $NSP4_{114–135}$-induced Cl^- secretion observed in the present study. Although intracellular Ca^{2+} is an essential factor for $NSP4_{114–135}$ activation of Cl^- secretion (as shown by inhibition of PLC with U73122 and ER-store depletion with CPA), additional and still unidentified factors may contribute. Interestingly, Cl^- secretion activated by CCH was not inhibited by inhibitors of PLC. Although there is no doubt that application of basolateral CCH enhances intracellular Ca^{2+} in mouse colon and activates basolateral SK4 K^+ channels [39], activation of luminal Cl^- channels by CCH appears largely independent of intracellular Ca^{2+}. Ca^{2+} influx pathways in colonic epithelial cells are not yet identified; however, Ca^{2+}-activated Cl^- secretion was unchanged in colon of mice lacking expression of TRPC1, TRPC4, or TRPC6, as well as in double and triple knockout animals (own unpublished data). Moreover, activation of Cl^- secretion was not affected by wortmannin or LY294002 (data not shown; [32]) and was, therefore, independent of PI3kinase. Finally, it cannot be ruled out that $NSP4_{114–135}$ binds directly to TMEM16A proteins to activate Cl^- secretion.

Multiple effects of NSP4 The present results point to the existence of multiple intracellular mechanisms by which $NSP4_{114–135}$ affects ion transport. Obviously, a PTX-sensitive G protein is activated, which increases PLC activity and causes depletion of ER-Ca^{2+} stores. NSP4 directly interacts with caveolin-1, the major structural protein of caveolae [30]. Similar to lipid rafts, caveolae organize signaling molecules at the plasma membrane, including phosphatidylinositol diphosphate (PIP_2), G proteins, ATPases, and Receptors [37]. NSP4 interacts with molecules localized in these functional microdomains, which promotes hydrolysis of PIP_2 and Ca^{2+} increase [31]. Accordingly, ENaC has been found to be compartmentalized in caveolin-rich lipid rafts, where it is regulated by caveolin-1 via a Nedd4-2-dependent mechanism [23]. It is, however, entirely possible that further, still unidentified signaling pathways are triggered that lead to activation of TMEM16A and inhibition of Na^+ absorption.

Along this line, PKC is activated (as demonstrated by the findings with B-oligomer of PTX and BIM) and is essential for the inhibitory effects on SGLT1 and ENaC. As shown earlier and in the present report, electrogenic Na^+-dependent glucose absorption by intestinal SGLT1 is potently inhibited by NSP4 [13]. SGLT1 inhibition by NSP4 and inhibition of ENaC are major disease-causing factors. Both genetic defects of SGLT1 as well as inhibition of ENaC during intestinal inflammation and tumor development are well known to cause profuse, fatal diarrhea [18, 22, 41, 43].

Lectin-type binding of NSP4 suggests a simple therapy for rotavirus induced diarrhea NSP4 binds to a protease sensitive plasma membrane receptor [9]. In the present study, we found that inhibition of G proteins by pertussis toxin inhibits the effects of $NSP4_{114–135}$ on Cl^- secretion but does not affect basolateral carbachol-induced Cl^- secretion. Binding of pertussis toxin through the B-oligomer subunit occurs through a lectin-like interaction, probably with sialic acid-

containing glycoconjugates located in the plasma membrane [14]. Binding of WGA has been shown to compete with B-oligomer binding [14], and it antagonizes the effects of $NSP4_{114–135}$, as demonstrated in the present study. While some lectins, such as concanavalin A, show clear effects on intestinal and airway electrolyte transport, this was not observed for other lectins such as WGA [21]. We suggest that WGA and maybe other phytohemagglutinins may be useful for the treatment of rotavirus infection, since it abrogates the pro-secretory responses of $NSP4_{114–135}$.

Along this line, WGA has been proposed for the treatment of cryptosporidiosis, and WG-containing supplements reduce cyst and trophozoite passage in people with giardiasis [11, 28]. Moreover, high-fiber diet appears to reduce the acute symptoms of giardia and helps to clear the infection. It is believed that the fibers induce mucous secretion and, in combination with bulk movement of insoluble fibers, reduced trophozoite attachment to the intestinal mucosa. However, reduced attachment may also be due to occupation of glycoconjugates by wheat agglutinins. Various approaches have been undertaken to develop novel antidiarrheal therapies. Thus, crofelemer, a proanthocyanidin oligomer, has been extracted as a natural compound from Croton Lechleri that inhibits both cAMP-activated CFTR as well as Ca^{2+}-activated TMEM16A Cl^- channels [40]. Lectin-conjugated glycine hydrazide (malonic hydrazides, MalH-lecins) have also been demonstrated to work as non-absorbable CFTR inhibitors, by membrane-anchoring the CFTR inhibitor to carbohydrates sitting on the surface of secretory colonic epithelial cells [38]. The present results suggest that competitive binding of dietary lectins may be beneficial in patients with rotavirus diarrhea. Taken together, the present work suggests that rotavirus-induced secretory diarrhea is due to activation of TMEM16A and parallel inhibition of Na^+ absorption. The pro-secretory effects of the rotavirus toxin NSP4 may be effectively antagonized by simple oral treatment with wheat germ agglutinin.

Acknowledgments This study is supported by the Deutsche Forschungsgemeinschaft DFG SFB699 A6/A7, DFG KU 756/8-2, and TargetScreen2 (EU-FP6-2005-LH-037365). KK was a research fellow of the University of Sydney Medical Foundation. We thank Dr. Brian Harfe and Dr. Jason Rock (University of Gainesville, Florida, USA) for supplying TMEM16A null mice and anti-mouse TMEM16A antibody and Ms. Marisa Sousa for her help with the TRPC-knockout animals.

References

1. Almaca J, Tian Y, AlDehni F, Ousingsawat J, Kongsuphol P, Rock JR, Harfe BD, Schreiber R, Kunzelmann K (2009) TMEM16 proteins produce volume regulated chloride currents that are reduced in mice lacking TMEM16A. J Biol Chem 284:28571–28578
2. Ball JM, Mitchell DM, Gibbons TF, Parr RD (2005) Rotavirus NSP4: a multifunctional viral enterotoxin. Viral Immunol 18:27–40
3. Ball JM, Tian P, Zeng CQ, Morris AP, Estes MK (1996) Age-dependent diarrhea induced by a rotaviral nonstructural glycoprotein. Science 272:101–104
4. Brunet JP, Cotte-Laffitte J, Linxe C, Quero AM, Geniteau-Legendre M, Servin A (2000) Rotavirus infection induces an increase in intracellular calcium concentration in human intestinal epithelial cells: role in microvillar actin alteration. J Virol 74:2323–2332
5. Buttery JP, Kirkwood C (2007) Rotavirus vaccines in developed countries. Curr Opin Infect Dis 20:253–258
6. Caputo A, Caci E, Ferrera L, Pedemonte N, Barsanti C, Sondo E, Pfeffer U, Ravazzolo R, Zegarra-Moran O, Galietta LJ (2008) TMEM16A, A Membrane Protein Associated With Calcium-Dependent Chloride Channel Activity. Science 322:590–594
7. Cook DI, Young JA (2002) Towards a physiology of epithelial pathogens. Pflügers Arch 443:339–343
8. de la Fuente R, Namkung W, Mills A, Verkman AS (2007) Small molecule screen identifies inhibitors of a human intestinal calcium activated chloride channel. Mol Pharmacol 73:758–768
9. Dong Y, Zeng CQ, Ball JM, Estes MK, Morris AP (1997) The rotavirus enterotoxin NSP4 mobilizes intracellular calcium in human intestinal cells by stimulating phospholipase C-mediated inositol 1, 4, 5- trisphosphate production. Proc Natl Acad Sci USA 94:3960–3965
10. Flores CA, Cid LP, Sepulveda FV (2010) Strain-dependent differences in electrogenic secretion of electrolytes across mouse colon epithelium. Exp Physiol 95:686–698
11. Grant J, Mahanty S, Khadir A, MacLean JD, Kokoskin E, Yeager B, Joseph L, Diaz J, Gotuzzo E, Mainville N, Ward BJ (2001) Wheat germ supplement reduces cyst and trophozoite passage in people with giardiasis. Am J Trop Med Hyg 65:705–710
12. Grubb BR (1999) Ion transport across the normal and CF neonatal murine intestine. Am J Physiol 277:G167–G174
13. Halaihel N, Lievin V, Ball JM, Estes MK, Alvarado F, Vasseur M (2000) Direct inhibitory effect of rotavirus NSP4(114–135) peptide on the Na(+)-D-glucose symporter of rabbit intestinal brush border membrane. J Virol 74:9464–9470
14. Heerze LD, Chong PC, Armstrong GD (1992) Investigation of the lectin-like binding domains in pertussis toxin using synthetic peptide sequences. Identification of a sialic acid binding site in the S2 subunit of the toxin. J Biol Chem 267:25810–25815
15. Keusch GT, Jacewicz M (1977) Pathogenesis of Shigella diarrhea. VII. Evidence for a cell membrane toxin receptor involving beta1 leads to 4-linked N-acetyl-D-glucosamine oligomers. J Exp Med 146:535–546
16. Kunzelmann K, Beesley AH, King NJ, Karupiah G, Young JA, Cook DI (2000) Influenza virus inhibits amiloride- sensitive Na^+ channels in respiratory epithelia. Proc Natl Acad Sci USA 97:10282–10287
17. Kunzelmann K, König J, Markovich D, King N, Karupiah G, Cook DI (2004) Acute effects of parainfluenza virus on epithelial electrolyte transport. J Biol Chem 279:48760–48766
18. Kunzelmann K, Mall M (2002) Electrolyte transport in the colon: Mechanisms and implications for disease. Physiol Rev 82:245–289
19. Kunzelmann K, Meanger J, King NJ, Cook DI (2007) Inhibition of airway Na^+ transport by respiratory syncytial virus. J Virol 81:3714–3720
20. Kunzelmann K, Scheidt K, Scharf B, Ousingsawat J, Schreiber R, Wainwright BJ, McMorran B (2006) Pseudomonas flagellin inhibits Na+ transport in airway epithelia. FASEB J 20:545–546
21. Kunzelmann K, Sun D, König J (2004) Effect of dietary lectins on ion transport in epithelia. Br J Pharmacol 142:1–8

22. Kunzelmann K, Sun J, Schreiber R, Konig J (2004) Effects of dietary lectins on ion transport in epithelia. Br J Pharmacol 142:1219–1226
23. Lee IH, Campbell CR, Song SH, Day ML, Kumar S, Cook DI, Dinudom A (2009) The activity of the epithelial sodium channels is regulated by caveolin-1 via a Nedd4–2-dependent mechanism. J Biol Chem 284(19):12663–12669
24. Lorrot M, Martin S, Vasseur M (2003) Rotavirus infection stimulates the Cl^- reabsorption process across the intestinal brush-border membrane of young rabbits. J Virol 77:9305–9311
25. Lorrot M, Vasseur M (2007) How do the rotavirus NSP4 and bacterial enterotoxins lead differently to diarrhea? Virol J 4:31
26. Morris AP, Estes MK (2001) Microbes and microbial toxins: paradigms for microbial-mucosal interactions. VIII. Pathological consequences of rotavirus infection and its enterotoxin. Am J Physiol 281:G303–G310
27. Morris AP, Scott JK, Ball JM, Zeng CQ, O'Neal WK, Estes MK (1999) NSP4 elicits age-dependent diarrhea and Ca^{2+} mediated I^- influx into intestinal crypts of CF mice. Am J Physiol 277:G431–G444
28. Moustafa MA (2003) Role of wheat germ agglutinin (WGA) in treatment of experimental cryptosporidiosis. J Egypt Soc Parasitol 33:443–456
29. Ousingsawat J, Martins JR, Schreiber R, Rock JR, Harfe BD, Kunzelmann K (2009) Loss of TMEM16A causes a defect in epithelial Ca^{2+} dependent chloride transport. J Biol Chem 284:28698–28703
30. Parr RD, Storey SM, Mitchell DM, McIntosh AL, Zhou M, Mir KD, Ball JM (2006) The rotavirus enterotoxin NSP4 directly interacts with the caveolar structural protein caveolin-1. J Virol 80:2842–2854
31. Pike LJ, Casey L (1996) Localization and turnover of phosphatidylinositol 4, 5-bisphosphate in caveolin-enriched membrane domains. J Biol Chem 271:26453–26456
32. Puntheeranurak S, Schreiber R, Spitzner M, Ousingsawat J, Krishnamra N, Kunzelmann K (2007) Control of ion transport in mouse proximal and distal colon by prolactin. Cell Physiol Biochem 19:77–88
33. Rock JR, Futtner CR, Harfe BD (2008) The transmembrane protein TMEM16A is required for normal development of the murine trachea. Dev Biol 321:141–149
34. Sausbier M, Matos JE, Sausbier U, Beranek G, Arntz C, Neuhuber W, Ruth P, Leipziger J (2006) Distal Colonic K^+ Secretion Occurs via BK Channels. J Am Soc Nephrol 17:1275–1282
35. Schreiber R, Uliyakina I, Kongsuphol P, Warth R, Mirza M, Martins JR, Kunzelmann K (2010) Expression and Function of Epithelial Anoctamins. J Biol Chem 285:7838–7845
36. Schroeder BC, Cheng T, Jan YN, Jan LY (2008) Expression cloning of TMEM16A as a calcium-activated chloride channel subunit. Cell 134:1019–1029
37. Shaul PW, Anderson RG (1998) Role of plasmalemmal caveolae in signal transduction. Am J Physiol 275:L843–L851
38. Sonawane ND, Zhao D, Zegarra-Moran O, Galietta LJ, Verkman AS (2007) Lectin Conjugates as Potent, Nonabsorbable CFTR Inhibitors for Reducing Intestinal Fluid Secretion in Cholera. Gastroenterology 132:1234–1244
39. Spitzner M, Ousingsawat J, Scheidt K, Kunzelmann K, Schreiber R (2007) Role of voltage gated K^+ channels for proliferation of colonic cancer cells. FASEB J 21:35–44
40. Tradtrantip L, Namkung W, Verkman AS (2009) Crofelemer, an antisecretory antidiarrheal proanthocyanidin oligomer extracted from croton lechleri, targets two distinct intestinal chloride channels. Mol Pharmacol 77:69–78
41. Wright EM (1993) The intestinal Na^+/glucose cotransporter. Annu Rev Physiol 55:575–589
42. Yang YD, Cho H, Koo JY, Tak MH, Cho Y, Shim WS, Park SP, Lee J, Lee B, Kim BM, Raouf R, Shin YK, Oh U (2008) TMEM16A confers receptor-activated calcium-dependent chloride conductance. Nature 455:1210–1215
43. Zeissig S, Bergann T, Fromm A, Bojarski C, Heller F, Guenther U, Zeitz M, Fromm M, Schulzke JD (2008) Altered ENaC expression leads to impaired sodium absorption in the noninflamed intestine in Crohn's disease. Gastroenterology 134:1436–1447
44. Zhang M, Zeng CQ, Dong Y, Ball JM, Saif LJ, Morris AP, Estes MK (1998) Mutations in rotavirus nonstructural glycoprotein NSP4 are associated with altered virus virulence. J Virol 72:3666–3672